

FCC to HCP transformation kinetics in a Co–27Cr–5Mo–0.23C alloy

R. Turrubiates-Estrada · A. Salinas-Rodriguez ·
H. F. Lopez

Received: 8 December 2009 / Accepted: 30 September 2010 / Published online: 14 October 2010
© Springer Science+Business Media, LLC 2010

Abstract In this work the kinetic aspects associated with the FCC → HCP martensitic transformation in a Co–27Cr–5Mo–0.23C alloy processed by powder metallurgy were investigated. In situ X-ray diffraction during isochronous heat treatments in a hot stage indicated that a fully metastable FCC matrix transforms rather fast at temperatures above 725 °C and reaches a maximum transformation into the HCP phase at 940 °C. Alternatively, when the matrix is HCP, some HCP martensite reverts to metastable FCC. Apparently, at low temperatures carbon excess in the HCP martensite promotes the reversal to metastable FCC. In addition, the volume percent of ε -martensite precipitated from stable FCC was determined as a function of time and temperature during isothermal aging between 675 and 900 °C. From these results, TTT diagrams were plotted for a 1% HCP transformed martensite. Maximum transformation rates were found to occur between 825 and 850 °C and activation energies, Q_s of 41–52 kcal/mol were estimated from the experimental outcome. The aged microstructures indicated that below 800 °C, the isothermal transformation was dominated by a lamellar morphology. Nevertheless, aging above 800 °C promoted carbide nucleation and coarsening along the grain boundaries independently of the FCC → HCP martensitic transformation.

Introduction

Cobalt-based (Co–Cr–Mo–C) alloys have been increasingly employed in the biomedical field due to their unique combination of mechanical strength, wear, and corrosion resistance [1–3]. In addition, the exhibited properties of these alloys can be improved through heat treatments aimed at controlling the relative volume fractions of microstructural components, including grain size [4]. In general, Co–Cr–Mo–C alloys exhibit two crystal structures, HCP and FCC, with HCP being thermodynamically stable at room temperature. However, the FCC to HCP transformation is difficult to achieve under normal cooling conditions and these alloys typically retain the high temperature FCC structure [4].

The FCC to HCP transformation can be induced athermally [4–6], isothermally [5–10], and through plastic straining [11, 12] with the resultant HCP phase known as ε -martensite. The athermal ε -martensite is induced by quenching from the FCC field of stability (typically above 1100 °C). Yet, the transformation is somewhat limited and it does not proceed beyond a volume fraction of 0.4–0.5 [13]. In contrast, isothermal aging after annealing at 1150 °C can lead to a complete FCC → HCP transformation when aging temperatures of the order of 650–950 °C are employed.

Kinetic investigations on the isothermal transformation indicate that during the FCC–HCP transformation carbides are concomitantly forming either at the advancing FCC–HCP interface or at grain boundaries (gbs) [5–10]. In addition, a discontinuous lamellar precipitation along the gbs has been observed which was attributed to a cellular precipitation reaction [14]. Apparently, in both low and high carbon versions of Co-based alloys continuous and discontinuous rows of minute carbides develop which tend to

R. Turrubiates-Estrada · A. Salinas-Rodriguez
Centro de Investigación y Estudios Avanzados del IPN Unidad
Saltillo, Carr. Saltillo-Monterrey km 13, 25900 Ramos Arizpe,
COAH, Mexico

H. F. Lopez (✉)
Materials Department, CEAS, University of Wisconsin–
Milwaukee, 3200 N. Cramer Street, Milwaukee, WI 53209, USA
e-mail: hlopez@uwm.edu

exhibit irregular (blocky) shapes or lamellar morphologies. In high carbon Co-based alloys, these carbides have been identified as $M_{23}C_6$ (FCC type) when they precipitate within the FCC matrix [15].

Carbide precipitation in the HCP matrix during the FCC \rightarrow HCP transformation has also been investigated in some detail for a high carbon wrought Co (0.18% C) based alloy [16]. In this case, it was found that carbides developed discontinuously at the FCC/HCP interface and it was assumed that they were $M_{23}C_6$ type. Yet, no conclusive experimental evidence was provided to show that this was indeed the case. Among other possible thermodynamically stable phases that can develop during isothermal aging is the σ phase [15, 17]. However, there are no reports which conclusively identify this phase in Co–Cr–Mo alloys.

From the kinetic studies [5–10], it has been found that the FCC to HCP transformation rates during isothermal aging are strongly influenced by the metallurgical condition, carbon content, and thermal processing. In general, depending on the annealing temperature and time, quenching to room temperature followed by aging can slow down the transformation kinetics. Internal and/or external stressing also hinders the transformation rates [11, 12]. Moreover, wrought alloys exhibit faster transformation kinetics when compared with cast alloys of similar carbon composition and similar heat treatments [10]. However, it is not clear why the FCC to HCP transformation is strongly influenced by the aforementioned factors.

Hence, in this work, an attempt is made to elucidate the role played by the carbon content, and by thermal processing. In particular, the transformation kinetics of a high carbon (0.23 wt% C) wrought Co–Cr–Mo alloy was investigated using in situ X-ray diffraction. Moreover, the equilibrium temperatures for the HCP and FCC phases were determined by these means.

Experimental

A powder metallurgy processed Co–27Cr–5Mo–0.23C alloy (Bio Dur Carpenter CCM) ASTM F-799 in bar shape was used in this work. The alloy had a grain size of 3.15 μm and the chemical composition is given in Table 1. The exhibited microstructures of the as-received (AR) and heat treated Co–Cr–Mo alloy conditions were characterized by metallographic means including optical and scanning electron microscopy (SEM).

Table 1 Chemical composition of as-received Co–Cr–Mo alloy

Element	Co	Mo	Cr	C	Ni	Fe	Mn	Si	P	W	S
Wt%	Bal	6.29	26.53	0.234	0.423	0.124	0.822	0.763	0.007	0.53	<0.002

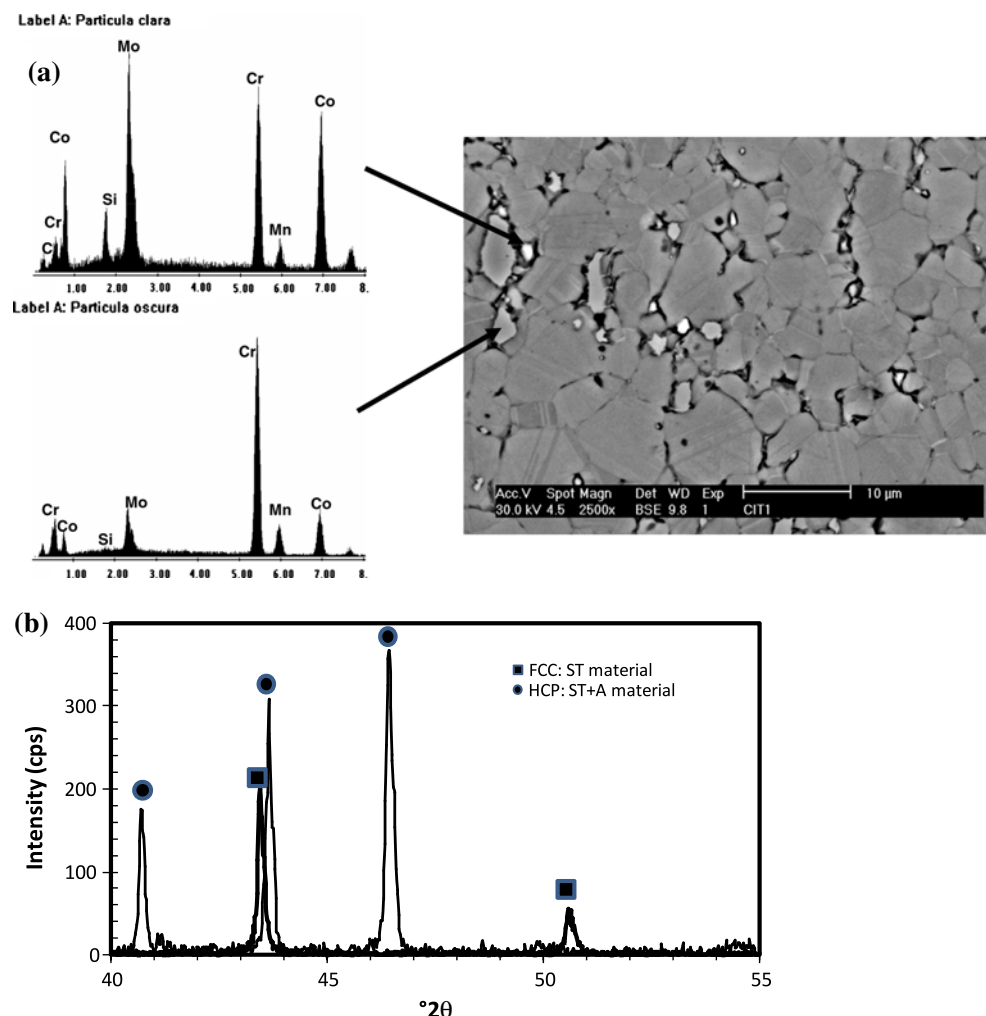
Samples of the AR cobalt alloy were solution treated (ST) at 1150 °C during 15 min and quenched into water at room temperature. This heat treatment produced a fully metastable FCC (FCC_m) structure. Some of the ST treated bars were subsequently aged (A) at 850 °C during 12 h to produce a structure consisting of 100% HCP at room temperature. The transformation behavior of the FCC_m and resultant HCP phases were followed by in situ X-ray diffraction during isochronous annealing of ST and A samples, respectively. The X-ray diffraction samples were 20 mm long, 10 mm wide, 0.5 mm thick and they were cut parallel to the bar cross-sections. Isochronous annealing was performed at temperature intervals of 40 °C from 625 to 1150 °C. At each temperature the alloy was isothermally annealed during 15 min and, simultaneously, the X-ray diffraction intensity was recorded between $40^\circ < 2\theta < 55^\circ$.

Similar samples were cut from the AR bars and used to follow the kinetics of the isothermal transformation from the metastable FCC phase (FCC_m) to HCP. Afterwards, the samples were heated at a rate of 1 °C/s to 1150 °C in the hot stage of the X-ray diffractometer and soaked during 15 min. After that, the samples were cooled at $-1^\circ \text{C}/\text{s}$ to aging temperatures between 675 and 950 °C. To ensure that the initial alloy structure at the beginning of aging was FCC_m , a set of samples were immediately quenched after reaching the aging temperatures and characterized by X-ray diffraction. Isothermal aging was carried out for up to 400 min and X-ray diffraction patterns between $40^\circ < 2\theta < 55^\circ$ were recorded at 15 min intervals. Within the $40^\circ < 2\theta < 55^\circ$ range the diffraction peaks that appear in the diffraction pattern are (111) and (200) for the FCC phase and (1010), (0002), and (1011) for the HCP phase. The relative weight fractions of HCP and FCC phases were determined using the integrated intensities of the (1011)_{HCP} and (200)_{FCC} peaks using the method proposed by Sage and Guillaud [18].

Results and discussion

Figure 1a shows the microstructural features of the Co-based alloy in the AR condition. The alloy was processed by powder metallurgy and exhibits some residual intrinsic porosity. Notice that the microstructure consists of a matrix of internally twinned equiaxed grains with second phases predominantly along the gbs. An evaluation of the chemical composition of the second phases present using

Fig. 1 **a** SEM micrograph of the Co-based alloy in the as-received condition including EDXS spectra of (Cr, Mo) and Cr rich carbides. **b** X-ray diffraction patterns of AR material obtained after a solution treatment (ST: 15 min at 1150 °C followed by water quenching) and after isothermal aging (A: 12 h at 850 °C)



energy dispersive X-ray spectrometry (EDXS) in the SEM indicated that these phases were probably alloyed carbides as they were Cr and Mo rich and they contained some carbon (see Fig. 1a). The X-ray diffraction patterns of the AR material obtained after a solution treatment (ST) and after isothermal aging (A) are shown in Fig. 1b. As can be seen, the ST material exhibits a fully FCC crystal structure while the ST + A material exhibits a fully HCP crystal structure.

Isochronous annealing

$FCC_m \rightarrow HCP$ transformation

Figure 2a and b is X-ray peak intensity profiles obtained during isochronous annealing of the Co–Cr–Mo–0.23C alloy with either an initial microstructure consisting of 100% FCC phase and 100% HCP, respectively. These diffraction peaks correspond to the various temperature–time intervals implemented all the way to 1150 °C. The relative amounts (wt%) of HCP phase transformed from

FCC_m calculated from the integrated intensities using the expression of Sage and Guillaud are graphically shown in Fig. 3. Notice from Figs. 2a and 3 that metastable FCC (FCC_m) slowly transforms to HCP at temperatures below 750 °C, but the transformation rates rapidly increase from 750 °C until at ~945 °C when the alloy structure becomes 100% HCP. It is noteworthy (see Fig. 3) that the $HCP \rightarrow FCC_s$ transformation starts at $T > 1025$ °C and ends at 1125 °C. Apparently, in the temperature range of 25–945 °C there is enough thermal energy to favor the $FCC_m \rightarrow HCP$ transformation.

According to the literature [19], the HCP phase is formed from metastable FCC via a martensitic reaction whose nucleation stage is thermally activated and can be rate limiting. Thus, the exponential trend exhibited by the $FCC_m \rightarrow HCP$ transformation at $T > 785$ °C (see Fig. 3) indicates that HCP nucleation is readily available for the transformation of the metastable FCC phase. At $T < 785$ °C, the activation of nucleation sites seems to be hindered by the lack of enough thermally activated dislocation maneuvers which will give rise to stable nuclei

Fig. 2 X-ray diffraction patterns in the Co-based alloy as a function of temperature for **a** an initial FCC matrix and **b** for a predominant HCP matrix

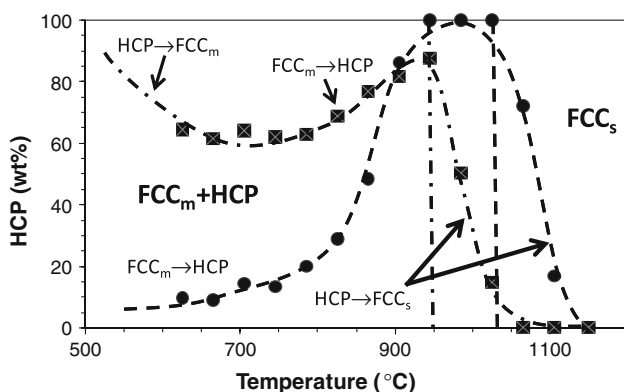
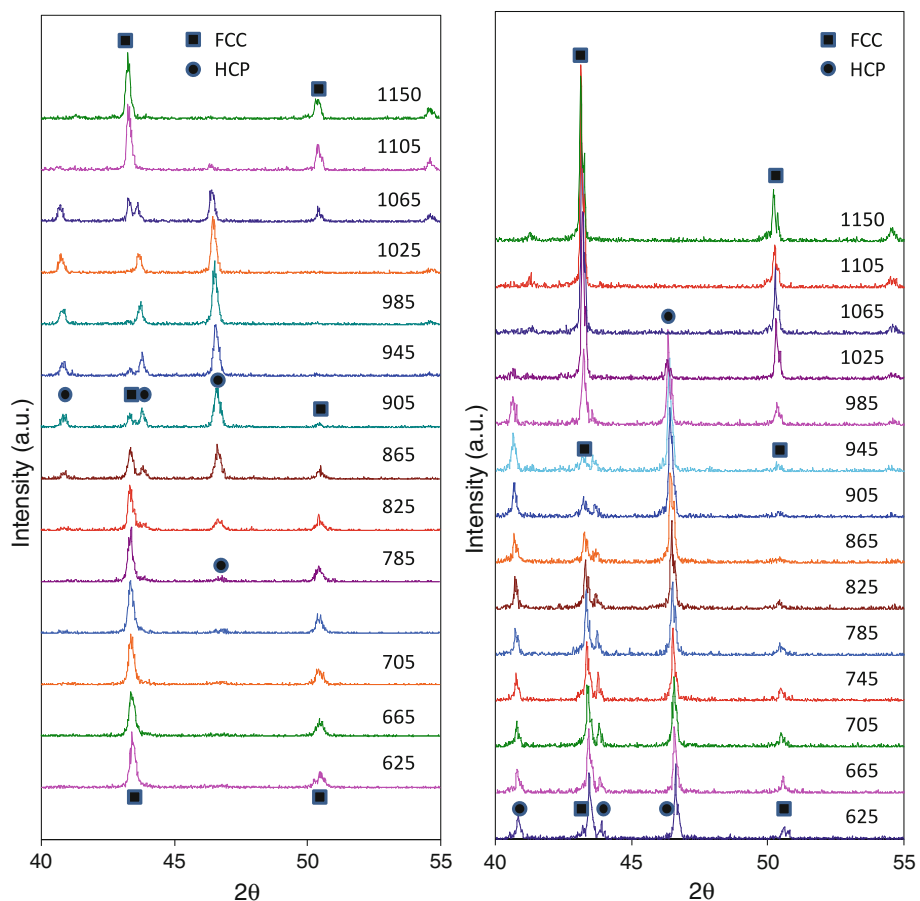


Fig. 3 Resultant volume percent transformation in isochronous heating for the Co-based alloy for the FCC \rightarrow HCP and HCP \rightarrow FCC transformation sequence

configurations [19]. Hence, only a relatively small number of nuclei participate of the transformation, accounting for the much slower transformation rates exhibited below 785 °C.

From Fig. 3, it is evident that the maximum temperature at which the FCC_m is present in the alloy microstructure is approximately 950 °C. Hence, it was decided to investigate the effects of temperature on the kinetics of the

FCC_m \rightarrow HCP during isothermal aging. The results are described in the following section, and they are compared with similar results obtained in a Co–27Cr–5Mo–0.05C alloy [6, 7] in an effort to understand the role of C in this transformation.

HCP \rightarrow FCC transformation

In the case of the alloy with a starting HCP crystal structure the transformation behavior is somewhat surprising. As shown in Figs. 2b and 3, during heating from room temperature, the HCP phase partially transforms to FCC_m with a maximum of 40% transformation at 700 °C. As the temperature is increased above 700 °C some of the newly formed FCC phase reverts to HCP until at about 950 °C when the HCP + FCC_m mixture rapidly transforms to FCC_s. According to the experimental data presented in Fig. 3, this transformation ends at approximately 1050 °C. Apparently, the presence of FCC_m during the transformation of the HCP phase accelerates the formation kinetics of the stable FCC phase in this alloy. In this case, it is not evident why metastable FCC should transform from the most stable HCP phase. A plausible explanation can be related to the development of local internal stresses within

the Co matrix. Internal stresses can arise from second phase precipitation reactions and/or thermal expansion differences between the FCC and HCP phases. In the work of Saldívar-García et al. [7, 20], it was found that the FCC → HCP transformation in a Co–27Cr–5Mo–0.05C alloy is accompanied by a contraction along the *c*-HCP axis. In turn, the stresses induced as a result of the thermal contraction along the basal planes might favor the formation of additional stacking faults and HCP martensite plates on (111) FCC planes.

Similar arguments can be used for precipitation reactions where the matrix surrounding the precipitates will be under compression. However, the development of these types of stresses is not able to explain the HCP to FCC transformation at temperatures much lower than the equilibrium HCP/FCC temperature.

Hence, a likely explanation is related to a possible carbon supersaturation of the initial HCP ϵ -martensite. It is well known that there is no measurable solubility of carbon in HCP cobalt [21] and during the FCC to HCP transformation carbon will tend to segregate at HCP embryos at defects such as partial dislocation cores in FCC stacking faults. In turn, this would lead to highly reduced dislocation mobilities and a retardation of the isothermal transformation.

Accordingly, at increasing temperatures above room temperature, some carbon-supersaturated ϵ -martensite plates might gain enough thermal energy to exhibit expansion and in this process give rise to metastable FCC. These arguments are supported by a similar experimental work carried out in a low carbon (0.05%) version of the Co–Cr–Mo alloy [6, 7]. In this work, no HCP transformation into metastable FCC was found at temperatures as high as 945 °C. Since, except for the C content, the alloy composition was similar to the one investigated in this work, it is apparent that the main differences are related to the carbon content which in turn can explain the experimental outcome of this work.

$FCC_m \rightarrow HCP$ transformation kinetics

Figure 4 shows peak intensity profiles obtained at room temperature of samples heated at a rate of 1 °C/s to 1150 °C in the hot stage of the X-ray diffractometer, soaked during 15 min, cooled at –1 °C/s to temperatures between 675 and 950 °C/s and finally cooled as fast as possible to room temperature. As can be seen, this type of heat treatment also produced structures consisting of 100% FCC_m , indicating that the structure of the alloy at the beginning of aging must also have been 100% FCC_m . Notice that no athermal ϵ -martensite was produced during cooling to room temperature.

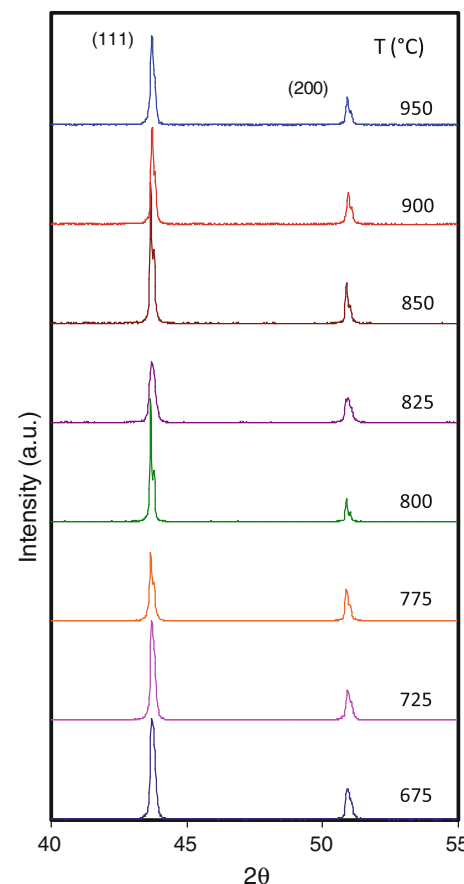


Fig. 4 X-ray diffraction patterns of Co–27Cr–5Mo–0.23C alloy solution treated for 15 min at 1150 °C, cooled at 1 °C/s to the indicated temperatures and then quenched to room temperature

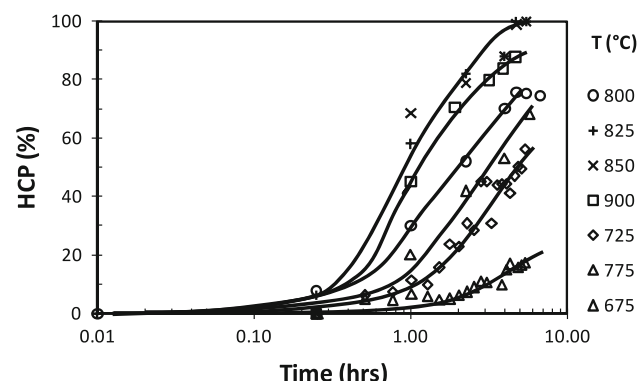


Fig. 5 Effect of temperature on the kinetics of the $FCC_m \rightarrow HCP$ transformation in Co–27Cr–5Mo–0.23C alloy solution treated during 15 min at 1150 °C and then cooled at 1 °C/s to isothermally aging temperatures between 675 and 900 °C

Figure 5 shows the effect of aging time on the amount of HCP martensite formed during isothermal aging at temperatures between 675 and 900 °C after cooling from 1150 °C. Notice that the transformation starts after an appreciable incubation period and follows an approximately sigmoidal

behavior as in previous works [5–10]. It is noteworthy that isothermal aging for up to 6 h produces a full transformation only at 825 and 850 °C and that the rate of transformation is slower during aging at lower or higher temperatures.

Figure 6 compares the kinetic data obtained at 825–850 °C with those reported by Saldívar-García et al. [6] on a low C (0.05%) Co–27Cr–5Mo alloy exposed to a similar heat treatment. As can be seen, in the high C alloy the incubation period is about four times longer and the average transformation rate is slower than in the low C content alloy. From the experimental outcome (data in Fig. 5), TTT curves were plotted as shown in Fig. 7. Maximum transformation rates (nose of TTT diagrams) were found between 800 and 850 °C. In the work of

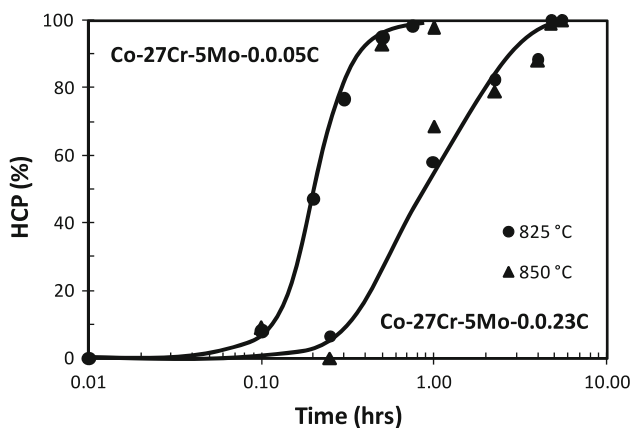


Fig. 6 Effect of C content on the kinetics of the $\text{FCC}_m \rightarrow \text{HCP}$ transformation in Co–27Cr–5Mo–0.23C alloy solution treated during 15 min at 1150 °C, cooled at 1 °C/s to 825–850 °C and isothermally aged at these temperatures. Comparison with Co–27Cr–5Mo–0.05C alloy, Ref. [6]

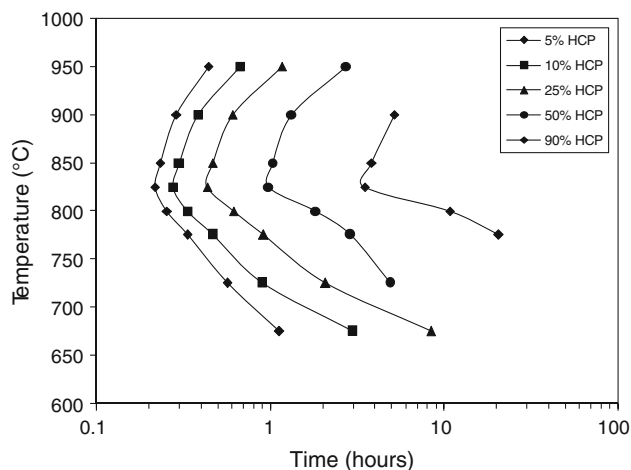


Fig. 7 TTT diagram for the $\text{FCC} \rightarrow \text{HCP}$ isothermal martensitic transformation in the investigated Co–Cr–Mo–C alloy

Saldívar-García et al. [6] maximum transformation rates were observed between 800 and 875 °C.

Resultant microstructures from the $\text{FCC}_m \rightarrow \text{HCP}$ transformation

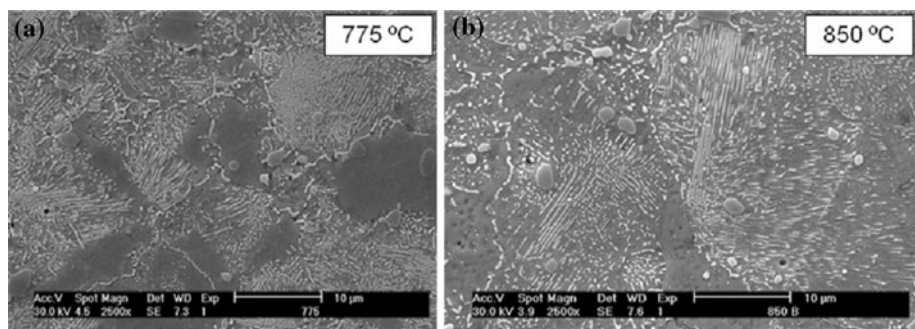
Figure 8a and b is SEM micrographs illustrating the microstructures of samples aged for 5.5 h at 775 and 850 °C, respectively. The amounts of HCP phase present in these microstructures are 68 and 100%, respectively (see Fig. 5). Notice that isothermal aging gives rise to a microstructure consisting of colonies of very fine, uniformly oriented, discontinuous lamellae resembling a pearlitic-type microstructure. Individual lamellae of irregularly shaped boundaries and various colonies with differently oriented lamellae can be observed within a given grain.

The morphology of the $\text{FCC}_m \rightarrow \text{HCP}$ transformation product illustrated in Fig. 8 is similar to that reported by Vander Sande et al. [5] in cast and wrought HS21 alloys aged 50 h at 650 °C, by Taylor and Waterhouse [15] in cast and solution treated Co–28.3Cr–5.4Mo–0.26C alloy aged between 750 and 1000 °C. Saldívar-García et al. [6, 7, 13] found similar microstructures in a low carbon solution treated Co–27Cr–5Mo–0.05C aged at temperatures between 650 and 950 °C. These workers also followed the microstructural changes as a function of aging time. Their results indicate that the lamellae appear to form preferentially at matrix/twin interfaces and gbs with no apparent compositional changes and sizes that do not increase with increasing aging times. They concluded that the $\text{FCC}_m \rightarrow \text{HCP}$ transformation proceeds by continuous nucleation of HCP lamellae.

As mentioned before, the sigmoidal shape of the transformation curves shown in Figs. 5 and 6 are similar to those observed by Saldívar-García et al. [6, 7] in a low carbon solution treated Co–27Cr–5Mo–0.05C aged at temperatures between 650 and 950 °C. This behavior is similar to the observations of Cong et al. [9] for the martensitic transformation during the isothermal aging of Co–27Cr–5.5Mo–0.25C alloy powders and by Rajan [14] for solution treated and quenched Co–26.7Cr–5.5Mo–0.15C alloy. The sigmoidal kinetics was explained in terms of thermally activated nucleation of HCP martensite where the rate limiting stage was the thermally activated motion of Shockley partial dislocations and their interaction with solute clusters.

In the higher carbon content alloys, small carbide particles were invariably found to have precipitated discontinuously in the newly formed HCP phase. In the Co–27Cr–5Mo–0.23C alloy investigated in this work, carbide precipitation was not detected by SEM and only the coarse Cr and Mo rich carbides observed in the solution

Fig. 8 SEM micrographs of the room temperature microstructures exhibited by samples annealed 15 min at 1150 °C, cooled and isothermally aged at **a** 775 °C and **b** 850 °C



treated condition (see Fig. 1) were observed in the aged microstructures (see Fig. 8). Apparently, the temperature of the solution treatment in the FCC phase stability field (1150 °C) was not highly enough and the aging times were relatively short to promote carbide dissolution. Therefore, carbide re-precipitation during cooling and aging is unlikely to have occurred in the present material. This conclusion is supported by the observations of Taylor and Waterhouse [15] and others that, in most Co–Cr–Mo–C alloys, carbide dissolution takes place at temperatures in excess of 1210 °C.

$FCC_m \rightarrow HCP$ transformation during isothermal aging

From the results described in the previous section it appears that increasing the C content from 0.05 to 0.23 wt% retards the kinetics of the $FCC_m \rightarrow HCP$ transformation in Co–27Cr–5Mo alloys subjected to a solution treatment at 1150 °C and then cooled and aged at temperatures between 675 and 950 °C. The apparent activation energy, Q , for the transformation was estimated at various temperatures using the following expression [22]

$$Q = -RT \ln\left(\frac{N_{0.05}}{nv}\right) \quad (1)$$

where n is the density of martensite nucleation sites (10^6 cm^{-3} taken from Magee [23]), v is the nucleation attempt frequency (10^{11} s^{-1} taken from Magee [23]), R is the universal gas constant, $N_{0.01}$ is the nucleation rate per volume for 0.01 transformation, and T is the absolute temperature. In addition, the average volume of transformed martensite plates, V can be calculated using the method of Fullman [24], where V is given by

$$V = \frac{\pi^2 f}{8EN_A} \quad (2)$$

In this equation, f is the volume fraction of martensite, E is the average of the reciprocal length of martensite plates as measured on a random cross-section, and N_A is the number of plates per unit area.

Figure 9 shows the rate of nucleation per volume ($N_{0.01}$) for temperatures in the range of 650–950 °C; maximum

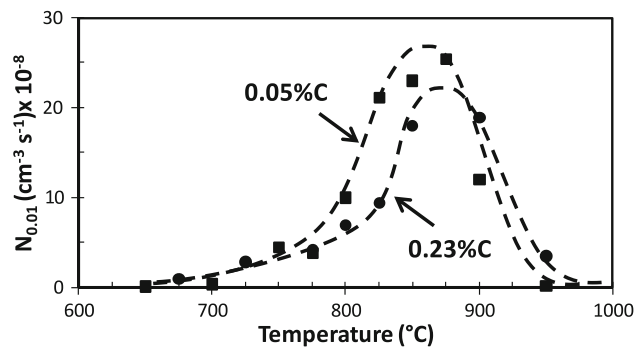


Fig. 9 Nucleation rates as a function of temperature during isothermal aging in the Co-based alloy. The alloy was previously annealed at 1150 °C for 15 min. Notice maximum nucleation rates at 825–850 °C and a comparison with Co–27Cr–5Mo–0.05C alloy, Ref. [6]

nucleation rates are observed between 850 and 875 °C. In addition, various activation energies were estimated as a function of temperature for this temperature range (see Fig. 9). Notice that the magnitudes of the exhibited activation energies tended to decrease slightly with increasing temperature in the range of 650–875 °C and then increase at higher temperatures. Despite these tendencies, the magnitudes of Q at temperatures between 650 and 950 °C (38 and 47 kcal/mol) are in good agreement with published reports [6, 7]. For comparison purposes, nucleation rate and activation energy data reported by Saldívar-García et al. [6] for a low C (0.05%) Co–27Cr–5Mo alloy are included in the graphs of Figs. 8 and 9, respectively. Notice that the increase in C content seems to have a limited effect both in $N_{0.01}$ and in Q .

The activation energies for the $FCC_s \rightarrow HCP$ transformation can be related to any active microstructural barriers for the split of lattice dislocations into Shockley partials. Olson and Cohen [25] attributed the transformation to be rate limited by the thermally activated motion of partial dislocations bounding a fault. Apparently, the ε -martensite transformation can be rate limited by the interaction between Shockley partials and short-range obstacles. In the work of Cong et al. [9], the short-range obstacles were considered to be mainly stacking fault intersections and solute clusters (Fig. 10).

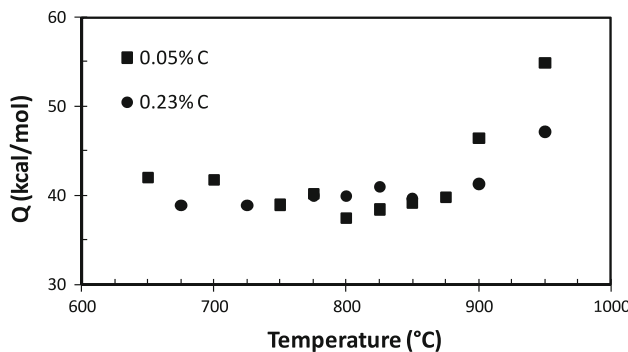


Fig. 10 Apparent activation energies determined as a function of temperature from measured volume fractions of ε -martensite in the Co-based alloy. Comparison with Co–27Cr–5Mo–0.05C alloy, Ref. [6]

In this work, the most likely solute which is expected to act as a short-range obstacle is carbon as it remains supersaturated in solid solution. Yet, as shown in Fig. 9, there is no significant influence of the carbon content on the activation energies when compared with those reported for a low carbon (0.05% C) Co-based alloy [6, 7].

Carbon effects

The FCC to HCP transformation kinetics has been investigated by various workers for Co–Cr–Mo–C alloys with various carbon contents and different processing conditions [5–10]. In general, the transformation kinetics seems to be delayed in cast Co-based alloys when compared with wrought ones of similar carbon contents and aging treatments [10]. Moreover, for similar annealing and aging conditions in Co-based alloys the transformation kinetics is hindered with increasing carbon contents [10]. Upon alloy cooling from the annealing temperatures, carbon remains in solid solution either at interstitial sites in the transformed HCP athermal martensite, or at the FCC metastable phase.

Since the carbon solubility in HCP cobalt is non-existent according to the phase diagram [21], it is expected that the stacking fault energy, γ will be increased significantly. From the point of view of Suzuki segregation, the effect of γ can be described by the existing interstitial chemical potentials μ_i , as well as solute and solvent chemical potentials [26]. In the limiting case of a pure metal under constant T and P , the γ dependence on μ_i can be described by [26].

$$d\gamma = -[\Gamma_i - (C_i/C_1)\Gamma_1]d\mu_i \quad (3)$$

where Γ_i is the surface excess of interstitials, Γ_1 is the surface excess of solvent, and C_i and C_1 are the mole fractions of interstitials and solvent, respectively. The above expression indicates that an atmosphere of interstitials can form on a fault, with the consequent modification in stacking fault energy. Accordingly, changes in the

stacking fault energy can lead to relatively high γ values depending on the local interstitial contents of carbon and nitrogen. However, there is no published data on Γ_i nor on the effect of interstitials on γ . In this work, the effect of interstitials on γ , particularly carbon could not be assessed. The experimental outcome indicates that carbon effects if any, should occur at levels of 0.05% or below as the exhibited Q does not differ much from the ones reported for low carbon versions [6, 7].

Additional evidence for the role of C on the FCC \rightarrow HCP transformation can be found by considering the development of ε -embryos from high temperature anneals and upon cooling to the aging temperatures. In this case, relatively small amounts of athermal martensite are exhibited after quenching (<12 vol.%), strongly suggesting that most of these embryos are unable to become active nuclei. Apparently, only a small fraction of embryos with relatively low γ 's are able to become effective sites for the development of athermal martensite [25]. Moreover, the Shockley dislocation partials which make the martensite embryos are not able to split indefinitely. In this case, the strain energy associated with the elastic fields of carbon-supersaturated partial dislocations might increase, as well as the coherency strains (i.e., deformation energy, associated with the HCP/FCC interphase [19]).

Conclusions

- A fully FCC matrix transforms rather fast at temperatures above 725 °C, reaching a maximum transformation into the HCP phase at 940 °C.
- When the matrix is fully HCP, some HCP martensite reverts to metastable FCC at temperatures below 625 °C.
- TTT diagrams were determined from determinations of volume percent of ε -martensite as a function of time and temperature during isothermal aging between 675 and 900 °C.
- Maximum isothermal transformation rates were found to occur at 825–850 °C.
- The exhibited activation energies for the isothermal transformation were of the order of 41–52 kcal/mol.
- A lamellar morphology was found to be predominant at the aging temperatures considered in this work.

References

1. Smethurst E, Waterhouse RB (1977) J Mater Sci 12:1781. doi: 10.1007/BF00566238
2. Rose RM (1974) Materials for internal prostheses. Yearbook of science and technology. McGraw Hill, New York

3. Buckley DH (1968) Cobalt 38:20
4. Huang P, Salinas-Rodriguez A, Lopez HF (1999) Mater Sci Technol 15:1324
5. Vander Sande JB, Coke JR, Wulff J (1976) Metall Trans A 7A:389
6. Saldívar-García AJ, Maní A, Salinas-Rodríguez A (1999) Metall Mater Trans A 30A:1177
7. Saldívar-García AJ (1998) Doctoral Thesis CINVESTAV-IPN Unidad Saltillo, Mexico
8. Rajan K, Vander Sande JB (1982) J Mater Sci 17:769. doi: [10.1007/BF00540374](https://doi.org/10.1007/BF00540374)
9. Cong Dahn N, Morphy D, Rajan K (1984) Acta Metall 32:1317
10. Lopez HF, Saldívar-García AJ (2008) Metall Mater Trans A 7A:389
11. Salinas-Rodriguez A, Rodriguez JL (1996) J Biomed Mater Res 31:409
12. Huang P (1997) Doctoral Thesis, University of Wisconsin-Milwaukee, USA
13. Saldívar-García AJ, Maní A, Salinas-Rodríguez A (1999) Scr Mater 40:717
14. Rajan K (1982) Metall Trans A 13A:1161
15. Taylor RNJ, Waterhouse RB (1986) J Mater Sci 21:1990. doi: [10.1007/BF00547938](https://doi.org/10.1007/BF00547938)
16. Lee SH, Takahashi E, Nomura N, Chiba A (1990) Mater Trans 47:287
17. Ramirez LE, Castro M, Mendez M, Lacaze J, Herrera M, Lesoult G (2002) Scr Mater 47:811
18. Sage M, Gillaud C (1950) Rev Met 49:139
19. Olson GB, Cohen M (1976) Metall Trans A 7A:1915
20. Saldívar-García AJ, López HF (2004) Metall Mater Trans A 35A:2517
21. Centre D'Information du Cobalt (1960) Cobalt Monograph, Belgium
22. Pati SR, Cohen M (1969) Acta Metall 17:189
23. Magee CL (1971) Metall Trans A 2A:2419
24. Fullman RL (1953) Trans Am Inst Min Eng 197:447
25. Olson GB, Cohen M (1975) Metall Trans A 6A:791
26. Hirth JP (1970) Metall Trans A 1A:2367